ACS OMEGA

Article

Cite This: ACS Omega 2018, 3, 12201−12214

http://pubs.acs.org/journal/acsodf

Effectiveness of Phytoactive Molecules on Transcriptional Expression, Biofilm Matrix, and Cell Wall Components of *Candida glabrata* and Its Clinical Isolates

Payal Gupta,[†] Sonam Gupta,[†] Meenakshi Sharma,[†] Navin Kumar,[‡] Vikas Pruthi,*[,†] and Krishna Mohan Poluri*[,†]

[†]Department of Biotechnology, Indian Institute of Technology Roorkee, Roorkee 247667, Uttarakhand, India

[‡]Department of Biotechnology, Graphic Era Deemed to be University, Dehradun 248002, Uttarakhand, India

Supporting Information

ABSTRACT: Toxicity challenges by antifungal arsenals and emergence of multidrug resistance scenario has posed a serious threat to global community. To cope up with this alarming situation, phytoactive molecules are richest, safest, and most effective source of broad spectrum antimicrobial compounds. In the present investigation, six phytoactive molecules [cinnamaldehyde (CIN), epigallocatechin, vanillin, eugenol (EUG), furanone, and epigallocatechin gallate] were studied against *Candida glabrata* and its clinical isolates. Among these, CIN and EUG which are active components of cinnamon and clove essential oils, respectively, exhibited maximum inhibition against planktonic growth of *C. glabrata* at a concentration of 64 and 128 μg mL^{-1}, respectively. These two molecules effectively inhibited and eradicated approximately 80% biofilm of *C. glabrata* and its clinical isolates from biomaterials. CIN and EUG increased reactive oxygen species generation, cell lysis, and ergosterol content in plasma membrane and reduced virulence attributes (phospholipase and proteinase) as well as catalase activity of *C. glabrata* cells. Reduction of mitochondrial membrane potential with increased release of cytochrome *c* from mitochondria to cytosol indicated initiation of early apoptosis in CIN- and EUG-treated *C. glabrata* cells. Transcriptional analysis showed that multidrug transporter (*CDR1*) and ergosterol biosynthesis genes were downregulated in the presence of CIN, while getting upregulated in EUG-treated cells. Interestingly, genes such as 1,3-β-glucan synthase (*FKS1*), GPI-anchored protein (*KRE1*), and sterol importer (*AUS1*) were downregulated upon treatment of CIN/EUG. These results provided molecular-level insights about the antifungal mechanism of CIN and EUG against *C. glabrata* including its resistant clinical isolate. The current data established that CIN and EUG can be potentially formulated in new antifungal strategies.

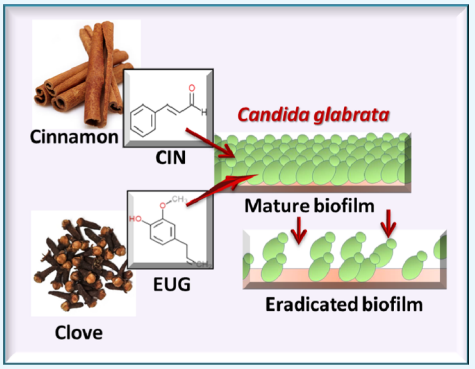

INTRODUCTION

Mortality and morbidity incidences of infections caused by *Candida* have increased in the last few decades. This escalating rate of infection depends upon a number of factors including age of the patient, antibiotic therapy, and immune state of patients.[1,2] In catheter-associated urinary tract infection, *Candida* is ranked second, whereas third is the blood-stream infections caused in intensive care unit.[3−5] Among *Candida* species, *Candida albicans* is the major etiological agent of invasive candidiasis in hospitalized patients. However, non-*albicans Candida* (NAC) species such as *Candida glabrata*, *Candida tropicalis*, and *Candida parapsilosis* have emerged as a leading cause of systemic candidiasis because of the arbitrary use of antibiotics and increased implanted devices.[6] In Australia, the incidence rate of *C. glabrata*-associated candidemia rose from 16 to 26.7% between 2004 and 2015.[7] The distribution of *Candida* species has changed in last decade resulting in an increase in proportion of *C. glabrata* in the U.S., Australia, and Europe, whereas *C. parapsilosis* in Latin America and Africa along with *C. albicans*.[8] In India, a total of 70 *Candida* isolates were collected in which *C. albicans* was present in 34 samples, whereas in 36 samples, predominant NAC spp. namely *C. tropicalis*, *Candida haemulonii*, *C. glabrata*, and *Candida pelliculosa* were found.[9] Similar reports related to incidences of candidiasis and dominance of NAC spp.-related infections are available from different parts of India, indicating the severity of fungal infections and their distribution.[10−12] Among NAC species, *C. glabrata* is highly infectious in immunocompromised, diabetic, and hematologic malignant patients.[13−17] It is also the major causative agent of vulvo vaginal candidiasis and candiduria.[18]

The recurrent infections caused by *Candida* spp. are difficult to treat because of their ability to form biofilm, a three-dimensional, complex architecture of surface-adhered cells

Received: August 1, 2018
Accepted: September 14, 2018
Published: September 28, 2018

DOI: 10.1021/acsomega.8b01856
ACS Omega 2018, 3, 12201−12214

encased into extracellular matrix (ECM) where microbes afford protected environment.[19] Cell surface hydrophobicity has an important role in cell adherence to substratum and is mediated by cell-surface-attached hydrophobic proteins.[20] Biofilm ECM is composed of exopolymeric substances in which the ratio of all macromolecules varies with the environment.[21] ECM acts as a barrier to toxic substances and drugs, protects cell from phagocytic cells, and maintains nutrients.[22] Also, it offer structural scaffold for cell adherence to different surfaces.[23] Extracellular DNA (eDNA) is also one of the important components of ECM and provides structural integrity.[24] The presence of hydrolytic enzymes (proteinase and phospholipase) in ECM facilitates tissue penetration and invasion.[25] Therefore, all of these characteristic features and components turn biofilm as a source of recalcitrant infections which are undoubtedly difficult to eradicate and hence liable for clinical repercussions.[26]

Sterol is an important component of eukaryotic cell membrane which is crucial for the structure maintenance and functioning of the cell. Ergosterol is a principal fungal sterol and a well-established target for three major classes of antifungals: azoles, polyenes, and echinocandin.[27,28] Any defect in ergosterol biosynthesis or drop in ergosterol content in *Candida* results in upregulation of *ERG* genes, *AUS1*, *TIR3* (sterol influx transporter), *SUT1*, and *UPC2* (sterol metabolism regulator).[29] *C. glabrata* is inherently resistant to azoles but a partial loss-of-function mutation in *MSH2* (DNA mismatch repair gene) is responsible for its unusual high resistance to azoles in clinical isolates.[2] Further, recent surveillance data have revealed the development of echinocandin resistance in *C. glabrata* because of mutations in hotspot regions of the genes *FKS1* and *FKS2*.[30] Echinocandin is the latest class of antifungal which was introduced 15 years back and till date a long pause in the discovery of clinically active antifungal reveals the hurdles associated with drug development for eukaryotic pathogens.[31]

Phytoactive molecules have emerged as a promising antibiofilm candidate which acts by inhibiting synthesis/degrading the signal molecule or blocking the binding site on receptor thereby, inhibiting the signal transduction cascade events.[32−34] Occurrence of phytoactive molecules has been reported in a variety of secondary metabolites (flavanoids and catechins) and essential oils (EOs).[35−37] EOs are plant-derived concentrated hydrophobic volatile liquids which serve as potential candidates for treating superficial infections.[38] They are well-documented antifungal agents and offer an advantage of being used in synergy with conventional antimycotics, even at a lower dose.[35,39,40] Earlier, reports on antifungal activity of phytoactive molecules have indicated their curative effect against *C. albicans*.[41] However, the role of phytoactive molecules on *C. glabrata* is still to be deciphered as it is different from *C. albicans* in terms of virulence, ploidy, size, phenotypic switching, and antifungal susceptibility.[42]

The present scenario of antifungal resistance against conventional therapies demands the need for more effective remedy against *C. glabrata* infections. The naturally occurring bioactive molecules stand out as potential therapeutic candidates against oral and superficial infections.[43] This study aimed to highlight the antifungal activity of six different phytoactive molecules, namely eugenol (EUG), epigallocatechin gallate, cinnamaldehyde (CIN), vanillin, furanone, and epigallocatechin (Figure 1), for their biofilm eradication potency and their effect on transcriptional expression, biofilm

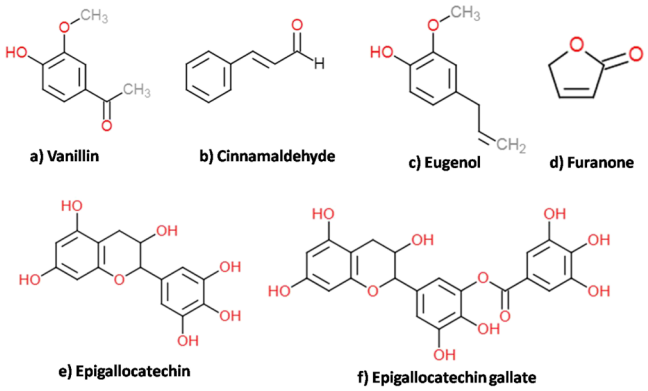

Figure 1. Chemical structure of phytoactive molecules. (a) Vanillin, (b) CIN, (c) EUG, (d) furanone, (e) epigallocatechin, and (f) epigallocatechin gallate. Chemical structures of the molecules were drawn using ChemDoddle software.

matrix, and cell wall components against *C. glabrata* and its clinical isolates. Of the selected phytoactive molecules, CIN and EUG are active components of EOs of cinnamon and clove, respectively, whereas catechins (epigallocatechin gallate and epigallocatechin) are derived from green tea. The phenolic compound vanillin is present in the vanilla pod extract, and furanone presence has been reported in red algae (*Delisea pulchra*).

RESULTS

Biofilm Formation Ability of *C. glabrata* and Its Clinical Isolates. The biofilm-forming ability of *C. glabrata* and its clinical isolates were compared at different time intervals (0−72 h) formed on 96-well microtiter plates (MTPs) and quantified using a 2,3-bis(2-methoxy-4-nitro-5-sulfo-phenyl)-2*H*-tetrazolium-5-carboxanilide (XTT) reduction assay (Figure 2). Data showed no significant difference

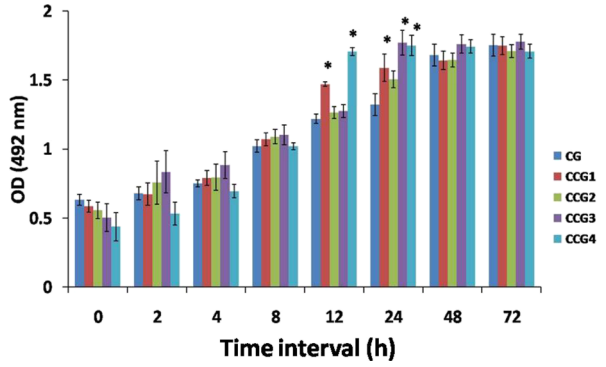

Figure 2. Comparative evaluation of *C. glabrata* and its clinical isolates biofilm development at different time interval (0−72 h). The value of XTT reduction assay at 492 nm is plotted with different time interval (*P < 0.05).

in surface adherence by *C. glabrata* and its clinical isolates on MTP, initially. However, results at 24 h biofilm of the clinical isolates CCG1, CCG3, and CCG4 were significantly higher (20, 33, and 30%, respectively; P < 0.05) to that of the control. Once the mature biofilm was formed after 48 h, again no considerable difference in the optical density (OD) values at 492 nm was recorded by XTT reduction assay (Figure 2).

DOI: 10.1021/acsomega.8b01856
ACS Omega 2018, 3, 12201−12214

Fungicidal Activity of Phytoactive Molecules. Planktonic growth inhibition of *C. glabrata* was recorded using six different phytoactive molecules (CIN, EUG, epigallocatechin gallate, vanillin, epigallacatechin, and furanone), as shown in Table 1. Among these, CIN and EUG having an MIC_{90} value of 64 and 128 $\mu g\ mL^{-1}$, respectively, were selected. These selected molecules were then tested against the growth of *C. glabrata* and its clinical isolates by performing a spotting assay. Data depicted fungicidal concentration of CIN and EUG to be 256 and 512 $\mu g\ mL^{-1}$, respectively, except CCG3 (Figure 3). Minimum fungicidal concentration (MFC) value of CIN was 512 $\mu g\ mL^{-1}$, whereas that of EUG was 1024 $\mu g\ mL^{-1}$ for CCG3, suggesting this clinical isolate to be the most resistant strain among the chosen isolates (Figure 3).

Table 1. MIC_{90} Value of Phytoactive Molecules for *C. glabrata* Planktonic Growth

s. no.	phytoactive molecules	source	MIC_{90} ($\mu g\ mL^{-1}$)
1	CIN	EO of cinnamon	64
2	EUG	EO of clove	128
3	EPG	leaf extract of green tea	512
4	vanillin	vanilla pod extract	>1024
5	EPC	leaf extract of green tea	512−1024
6	furanone	extract of red algae	512−1024

Inhibitory and Eradication Potency of CIN and EUG. The biofilm inhibitory and eradication potency of CIN and EUG were checked against *C. glabrata* and its clinical isolates (Figures S1 and S2; Table 2). The results were expressed as biofilm inhibitory concentration (BIC_{80}) and biofilm eradication concentration (BEC_{80}). The inhibition of *C. glabrata* and its clinical isolate biofilm were gradual with increasing concentration of CIN from 0 to 512 $\mu g\ mL^{-1}$. Enhanced percent inhibition of biofilm was recorded in EUG when the concentration was raised from 32 to 512 $\mu g\ mL^{-1}$ (Figure S1). The BIC_{80} value of CIN for *C. glabrata* and its clinical isolate (except CCG3) was 64 $\mu g\ mL^{-1}$, whereas it was 128 $\mu g\ mL^{-1}$ for CCG3, suggesting that clinical isolate CCG3 to be more surface adhering and less susceptible to CIN and EUG (Table 2). EUG also exhibited similar inhibition pattern; BIC_{80} value of CCG3 (256 $\mu g\ mL^{-1}$) was twice the BIC_{80} value for all strains (128 $\mu g\ mL^{-1}$). The biofilm susceptibility of *C. glabrata* and its clinical isolates toward CIN were higher (2× times) than that of EUG (Table 2).

Efficacy of CIN and EUG in eradicating *C. glabrata* and its clinical isolate biofilm was examined in 96-well MTPs using XTT reduction assay (Table 2; Figure S2). The BEC_{80} value of CIN for all strains was 128 $\mu g\ mL^{-1}$ except CCG1 and CCG2 for which it was twofold lower (64 $\mu g\ mL^{-1}$), as shown in Table 2. The BEC_{80} value of CIN for CCG1, CCG2, and CCG3 were similar to their respective BIC_{80}, whereas that of *C. glabrata* and CCG4, it was twofold higher than their BIC_{80}, indicating less susceptibility of their mature biofilm. The BEC_{80} value of EUG for *C. glabrata*, CCG1, and CCG3 was 512 $\mu g\ mL^{-1}$, whereas it was 256 $\mu g\ mL^{-1}$ for CCG2 and CCG4, indicating sensitivity of mature biofilm of CCG2 and CCG4 toward EUG (Table 2; Figure S2).

Table 2. BEC_{80} and BIC_{80} of CIN and EUG Against *C. glabrata* and Its Isolates

	CIN ($\mu g\ mL^{-1}$)		EUG ($\mu g\ mL^{-1}$)	
strain	BIC_{80}	BEC_{80}	BIC_{80}	BEC_{80}
C. glabrata	64	128	128	512
CCG1	64	64	128	512
CCG2	64	64	128	256
CCG3	128	128	256	512
CCG4	64	128	128	256

The biofilm inhibitory effect of CIN and EUG can be correlated with the results of surface hydrophobicity index (HI) of CIN- and EUG-treated *C. glabrata* and CCG3 which was measured by a two-phase system. The HI value showed that CCG3 (90%) was significantly more hydrophobic than *C. glabrata* (71%). The hydrophobicity of CIN (68.4%)- and EUG (65.34%)-treated *C. glabrata* decreased as compared to control. Whereas the HI value of CCG3 treated with CIN (35.0%) decreased but remain unchanged when exposed to EUG (84.3%) (Figure S3).

Effect of CIN and EUG on *C. glabrata* Extracellular Matrix. The effect of CIN and EUG treatment on biochemical composition of *C. glabrata* extracellular matrix (ECM) was studied and compared with that of CCG3. The carbohydrate content of ECM in control, *C. glabrata,* and CCG3 control were almost similar. An increase in the carbohydrate content of ECM was observed in both *C. glabrata* (30%) and CCG3 (26%) upon CIN exposure, as compared to their respective control (Figure 4A). However, no change in carbohydrate content was noticed upon EUG treatment. Indeed, no change was observed in the protein content and eDNA content of CIN- and EUG-treated *C. glabrata* and CCG3 ECM (Figure 4B,C).

The enzymatic activity of *C. glabrata* ECM treated with CIN and EUG was also studied. Proteinase activity was found to be higher in CCG3 as compared to *C. glabrata*. However, in the presence of CIN and EUG, the proteinase activity decreased in both *C. glabrata* and CCG3 (Figure 4D). Likewise, the

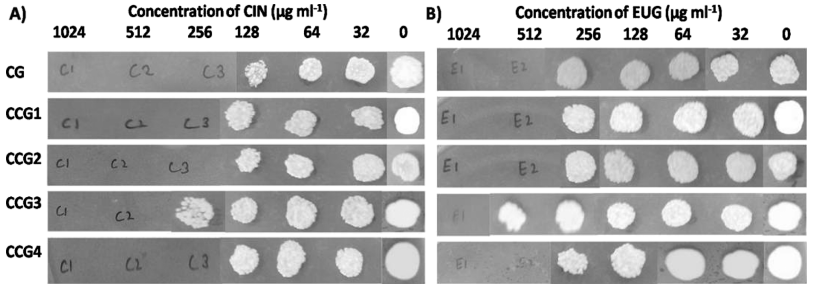

Figure 3. MFC of CIN (A) and EUG (B) against planktonic growth of *C. glabrata* and its isolates on YPD media plates after 48 h of preincubation in RPMI medium with phytoactive molecules.

DOI: 10.1021/acsomega.8b01856
ACS Omega 2018, 3, 12201−12214

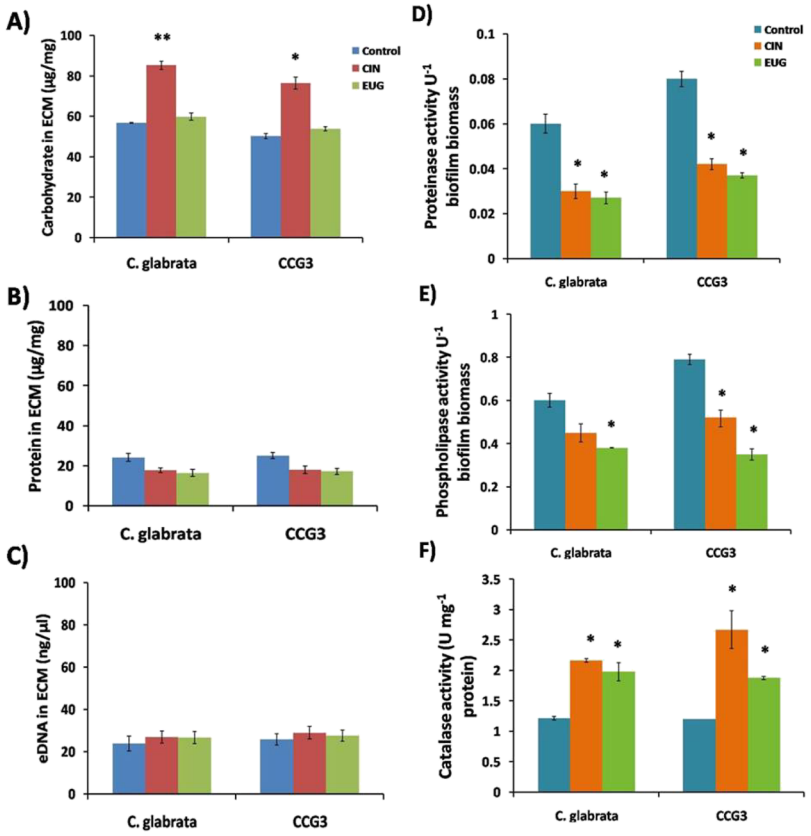

Figure 4. Quantification of biochemical composition (A) carbohydrate; (B) protein and (C) eDNA in ECM and the specific activity of the enzymes (D) proteinase; (E) phospholipase and (F) catalase activity in *C. glabrata;* and CCG3 biofilm exposed to CIN (128 μg mL^{-1}) and EUG (256 μg mL^{-1}) after 48 h. Data represent means ± SDs of three independent experiments (**P < 0.01 and *P < 0.05).

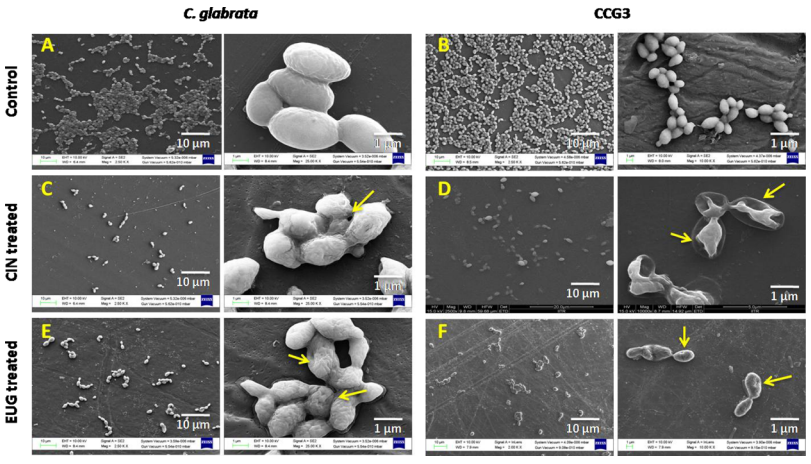

Figure 5. FESEM images of 48 h mature *C. glabrata* (A) and CCG-3 biofilm (D); after 24 h of treatment with 128 μg mL^{-1} CIN (B,E); and 256 μg mL^{-1} EUG (C,F). The scale bar of magnification is 10 μm/1 μm.

phospholipase activity of CIN- and EUG-treated *C. glabrata* and CCG3 ECM was reduced (Figure 4E). The catalase activity of untreated *C. glabrata* and CCG3 was same, whereas in the presence of CIN and EUG, the activity increased 2- and 1.8-fold, respectively, for both *C. glabrata* and CCG3 (Figure 4F).

Above observations suggested that biochemical composition and enzymatic activity of *C. glabrata* and CCG3 ECM were affected by CIN and EUG in a similar manner. As expected, in CCG3 control samples, the hydrolytic enzyme activity (phospholipase and proteinase) was more as compared to *C. glabrata* control cells. However, no noticeable change was observed in catalase activity between control and CCG3.

Assessment of Morphological Changes in *C. glabrata* Biofilm. Morphological analysis of *C. glabrata* and CCG3 biofilm samples at BEC_{80} value of CIN and EUG was performed on polystyrene disc (1 cm^2) for 48 h using field-emission scanning electron microscopy (FESEM). The biofilm of untreated *C. glabrata* and CCG3 retained their structural integrity as healthy yeast cells (Figure 5A,B). CCG3 exhibited substantial cell-rupturing features as compared to *C. glabrata* upon treatment of CIN. CCG3 cells depicted sunken and

DOI: 10.1021/acsomega.8b01856
ACS Omega 2018, 3, 12201−12214

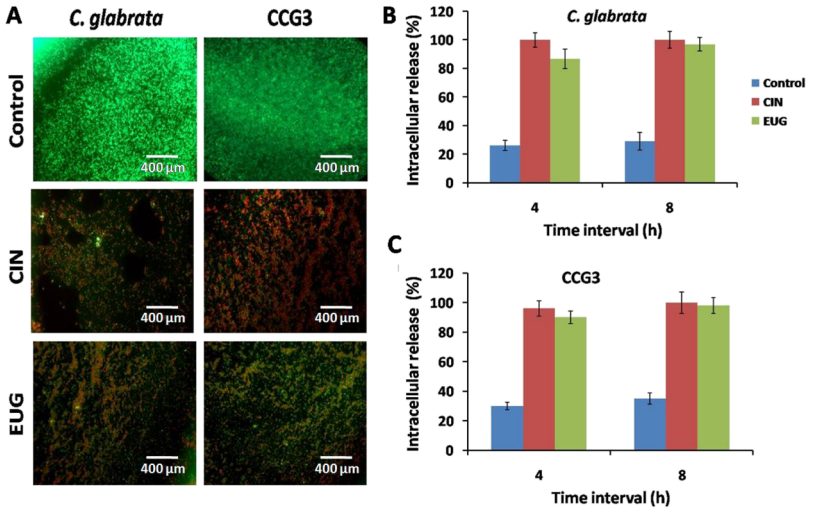

Figure 6. (A) Fluorescence microscopy of 48 h mature *C. glabrata* and CCG3 biofilm after treatment with CIN (128 μg mL^{-1}) and EUG (256 μg mL^{-1}) stained with FDA + PI. Scale bar represents 400 μm. Quantification of intracellular material release in *C. glabrata* and CCG3 cells treated with (B) CIN (128 μg mL^{-1}) and (C) EUG (256 μg mL^{-1}).

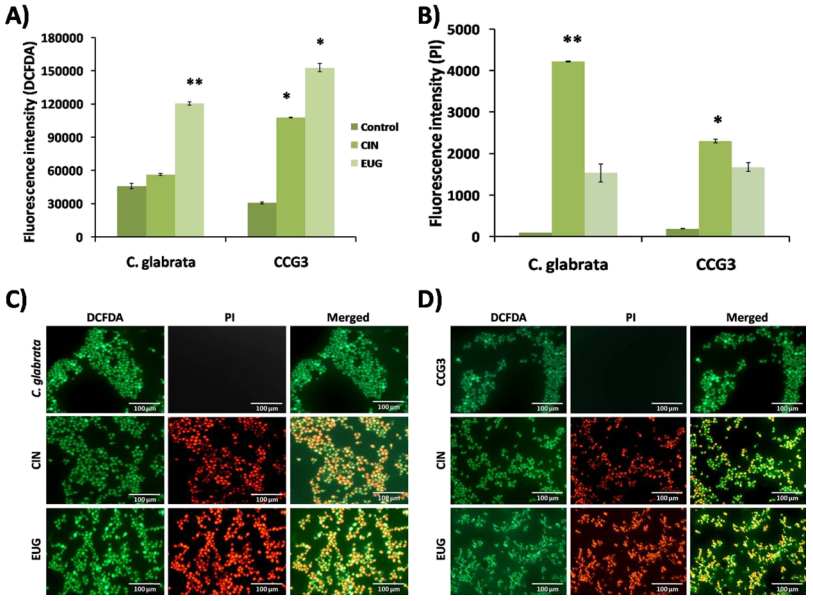

Figure 7. Amount of ROS accumulation in terms of fluorescence intensity of (A) DCFDA and (B) PI in *C. glabrata* and CCG3 biofilms exposed to CIN (128 μg mL^{-1}) and EUG (256 μg mL^{-1}) after 48 h. Fluorescence microscopy images of ROS generation in (C) *C. glabrata* and (D) CCG3 biofilm for the detection of ROS (green), cell lysis (bright red), and eDNA (diffuse red). The scale bar represents 100 μm.

shrunk cellular features and are separated from outer cell wall (Figure 5C,D). However, EUG treatment on both *C. glabrata* and CCG3 biofilm depicted pore formation with wrinkled topology (Figure 5E,F).

To assess the cellular damage caused by CIN and EUG to *C. glabrata* biofilm cells, fluorescence microscopy was performed to visualize live−dead cells by FDA−PI. All metabolically active cells emit diffusely distributed green fluorescence, whereas those with damaged membrane showed red fluorescence. In FDA−PI stained biofilm, control emitted only green fluorescence which indicated live cells, whereas CIN- and EUG-treated *C. glabrata* and CCG3 biofilm emitted red−green fluorescence (Figure 6A).

To further co-relate the observations of fluorescence microscopy, the effect of CIN and EUG on cell membrane was determined in terms of rate and amount of released nucleic acid from *C. glabrata* and CCG3 cells (Figure 6B,C). Both CIN and EUG caused approximately 90% nucleic acid release in *C. glabrata* and CCG3 after 4 h of incubation. Hundred percent cell lysis was observed after 8 h of incubation of cells with CIN and EUG. Hence, the cell lytic effect of CIN and EUG on *C. glabrata* and CCG3 can be interpreted.

Reactive Oxygen Species Generated When Cells Exposed to CIN and EUG. Two fluorogenic dyes, 2′,7′-dichlorodihydrofluorescein diacetate (DCFDA) and PI, were used for reactive oxygen species (ROS) study; DCFDA measure ROS level inside the cell, whereas PI showed cell lysis by binding the DNA. Increased level of intracellular ROS accumulation was recorded in the presence of EUG but not in CIN-treated *C. glabrata,* whereas the level of ROS accumulation was increased in CCG3 cells upon both, CIN and EUG exposure (Figure 7A). The damaging effect of ROS

DOI: 10.1021/acsomega.8b01856
ACS Omega 2018, 3, 12201−12214

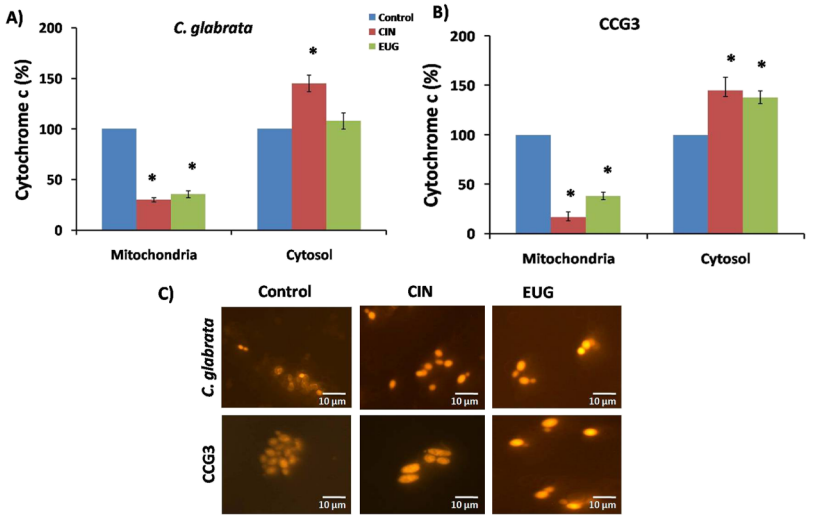

Figure 8. Release of cytochrome *c* from mitochondria to cytoplasm in response to CIN (128 μg mL^{-1}) and EUG (256 μg mL^{-1}) treatment in (A) *C. glabrata* and (B) CCG3. (C) Fluorescence microscopy of *C. glabrata* and CCG3 cells stained with rhodamine B to study the effect of CIN (128 μg mL^{-1}) and EUG (256 μg mL^{-1}) on MMP. Images were taken at 60× magnification. The scale bar represents 10 μm.

accumulation on cells was demonstrated in terms of the binding ability of PI to DNA of the lysed cells, and the fluorescence intensity of bounded PI was found to be higher in CIN-exposed cells (Figure 7B). Fluorescence microscopy images of CIN/EUG treated and untreated cells depict red and green fluorescence indicating dead and live cells, respectively (Figure 7C,D).

Cytochrome *c* Release into Cytosol and Mitochondrial Membrane Potential. Cytochrome *c* content was measured in mitochondria and cytosol of CIN and EUG treated *C. glabrata* and CCG3 because it gives an indirect evidence of apoptosis. In *C. glabrata* cells, cyt *c* release was increased from 25 to 145 and 38 to 108% in the presence of CIN and EUG, respectively, from mitochondria to cytosol (Figure 8A). Similarly, in CIN- and EUG-treated CCG3 cells, cyt *c* was released from 14 to 140 and 38 to 133%, respectively (Figure 8B).

The change in MMP of CIN (128 μg mL^{-1}) and EUG (256 μg mL^{-1}) treated log phase *C. glabrata,* and CCG3 cells was analyzed by fluorescent cationic rhodamine B dye using a fluorescent microscope. The effect of CIN and EUG treatment on ATP production in *C. glabrata* cells was determined indirectly by measuring MMP using rhodamine B (Figure 8C). Rhodamine B, a hexyl ester, emits red fluorescence which in response to transmembrane potential distributes itself across biological membrane. CIN and EUG treatment increased the MMP, making the membrane more negatively charged which resulted in more accumulation of rhodamine B as compared to untreated control *C. glabrata* and CCG3. Collectively, cyt *c* quantification and MMP data depict the role of CIN and EUG in mediating early apoptosis.

CIN and EUG Differentially Modulate Transcriptional Expression. The ergosterol content in plasma membrane of CIN-and EUG-treated *C. glabrata* and CCG3 was quantified spectrophotometrically. No noticeable change in the ergosterol content was observed on CIN-treated *C. glabrata* cells. A significant increase in the ergosterol content was observed upon EUG treatment in both *C. glabrata* and its clinical isolate CCG3 (Figure 9). Furthermore, the enhancement of ergosterol in CCG3 is higher to that of the reference strain.

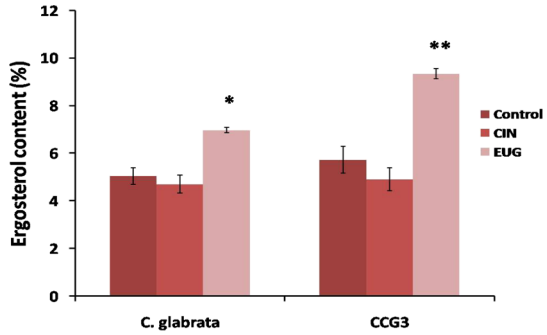

Figure 9. Ergosterol content as percent wet weight of *C. glabrata* and CCG3 in CIN (32 μg mL^{-1}) and EUG (64 μg mL^{-1}) untreated and treated cells (**P < 0.01 and *P < 0.05).

To gain insights into the mechanism of action of CIN and EUG against *C. glabrata* and CCG3 growth, transcriptional analysis of ergosterol synthesis genes (*ERG2*, *ERG3*, *ERG4*, *ERG10*, and *ERG11*), sterol importer (*AUS1*), GPI-anchored cell wall protein (*KRE1*), 1,3-β-glucan synthase (*FKS1*), and multidrug transporter (*CDR1*) genes were investigated by qRT-PCR, as summarized in Table S1. Expression levels of *AUS1*, *KRE1*, and *FKS1* were significantly downregulated upon treatment of both CIN/EUG. However, the expression levels of ergosterol synthesis genes showed differential behavior upon treatment of CIN/EUG. Upon CIN treatment, *ERG2*, *ERG4*, and *ERG11* were moderately downregulated, whereas *ERG10* was moderately upregulated. In case the of EUG upregulation of *ERG2*, *ERG3*, *ERG10*, and *ERG11*, *CDR1* was observed (Table 3).

Biofilm Eradication from Clinically Relevant Biomaterials. To investigate the biofilm eradication of *C. glabrata* and CCG3 by CIN and EUG formed on the surface of clinically relevant biomaterials (silicone urinary catheter and contact eye lens), XTT reduction assay was performed. The absorbance values of XTT reduction assay at 492 nm indicated that the clinical isolate CCG3 formed three times more biofilm as compared to *C. glabrata* on urinary catheters indicating thereby that the CCG3 strain was more pathogenic/virulent because of its stronger adhering properties on biomaterial

DOI: 10.1021/acsomega.8b01856
ACS Omega 2018, 3, 12201−12214

Table 3. CG and CCG3 Genes Up- and Downregulated in Response to Subinhibitory Concentration of CIN (32 μg mL^{-1}) and EUG (64 μg mL^{-1}) and EUG[a]

		fold expression				
		C. glabrata		CCG3		
C. glabrata (ORF status)	*S. cerevisiae* homologue	CIN	EUG	CIN	EUG	description
CAGL0M01760g (verified)	*CDR1*	−1.4	1.84	−1.13	2.4	ABC multidrug transporter regulated by Pdr1p
CAGL0L10714g (uncharacterized)	*ERG2*	−1.67	1.3	−1.4	2.1	C-8 sterol isomerase
CAGL0F01793g (verified)	*ERG3*	−1.4	2.7	−2.12	4.2	C-5 sterol desaturase
CAGL0A00429g (uncharacterized)	*ERG4*	−3.34	−1.11	−2.0	−1.25	C-24 sterol reductase
CAGL0L12364g (uncharacterized)	*ERG10*	2.3	2.0	3.4	3.7	acetyl-CoA C-acetyltransferase have role in sterol biosynthesis
CAGL0E04334g (verified)	*ERG11*	−1.64	1.7	−1.4	2.6	cytochrome P-450 lanosterol 14-alpha-demethylase role in ergosterol synthesis
CAGL0F01419g (verified)	*AUS1*	−52	−20.0	−7.14	−5.55	ABC transporter involved in sterol uptake
CAGL0M04169g (uncharacterized)	*KRE1*	−16.39	−20.4	−18.86	−12.19	role in cell wall biogenesis and organization
CAGL0G01034g (verified)	*FKS1*	−50.0	−7.24	−25.0	−4.76	component of 1,3-beta-glucan synthase

[a]Genes showing a fold expression ≥1.5 were only considered to assess the changes. Fold expression of 1.5−5.0 are considered as moderate expression, and those showing a change ≥5.0 are considered to be significant.

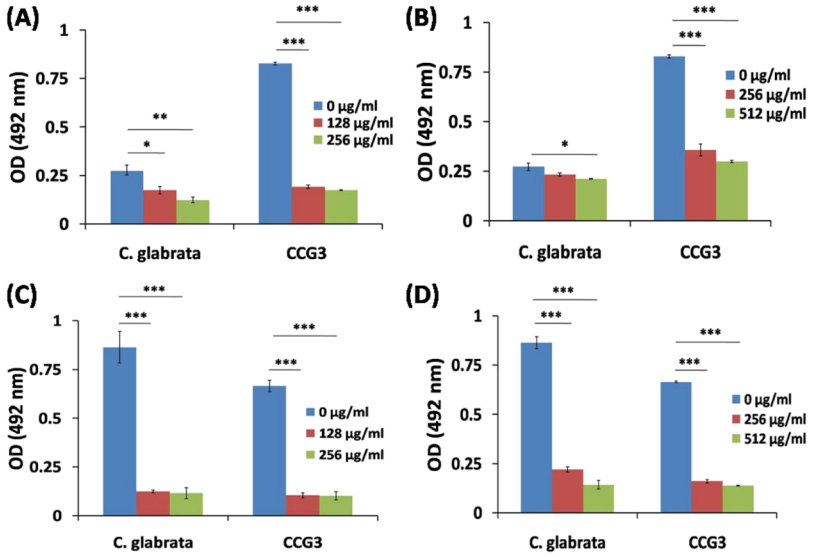

Figure 10. Quantification of *C. glabrata* and CCG3 biofilm developed on urinary catheter (A,B) and contact eye lens (C,D) after treatment at different concentrations of CIN (A,C) and EUG (B,D).

devices (Figure 10). Both CIN and EUG showed eradication of *C. glabrata* and CCG3 biofilm from the urinary catheter (Figure 10A,B). CIN at a concentration of 256 μg mL^{-1} eradicated ∼55% of *C. glabrata* biofilm from the urinary catheter, whereas EUG showed ∼23% eradication of *C. glabrata* biofilm at 512 μg mL^{-1} (Table S2). However, CIN has eradicated more than 75% of CCG3 biofilm at a concentration of 256 μg mL^{-1}, whereas EUG eradicated 64% CCG3 biofilm from the urinary catheter (Table S2). This suggests that CIN and EUG to be a potent antifungal against clinical isolate CCG3 biofilm. The differences in the eradication of CIN and EUG between *C. glabrata* and CCG3 can be attributed to their differential adherence properties on silicone urinary catheters.

C. glabrata and CCG3 formed almost similar amount of biofilm on contact eye lens with OD values 0.86 (CG) and 0.67 (CCG3), suggesting the contact lens to be good surface-adhering biomaterial. CIN and EUG have eradicated a biofilm of *C. glabrata* and CCG3 to a significant extent from the contact eye lens (Figure 10C,D). CIN (256 μg mL^{-1}) and EUG (512 μg mL^{-1}) showed a maximum eradication of *C. glabrata* biofilm from the eye lens (86.6 ± 2.5 and 83.7 ± 2.8%) at their highest concentrations (Figure 10C,D; Table S2).

DISCUSSION

Candida is an opportunistic commensal fungal pathogen known to cause superficial to systemic infections. The aptitude of these pathogens to form biofilm is a prime virulence trait responsible for their multidrug resistance which often leads to failure of therapeutic strategies.[44] Biofilm is a structured community of harmonically communicating sessile cells encapsulated in ECM.[34] Disintegration of this irreversible structure is a powerful target for therapeutic intervention. Screening of traditional medicine which can reduce biofilm is a promising approach in modern era.[45] The antimicrobial

DOI: 10.1021/acsomega.8b01856
ACS Omega 2018, 3, 12201−12214

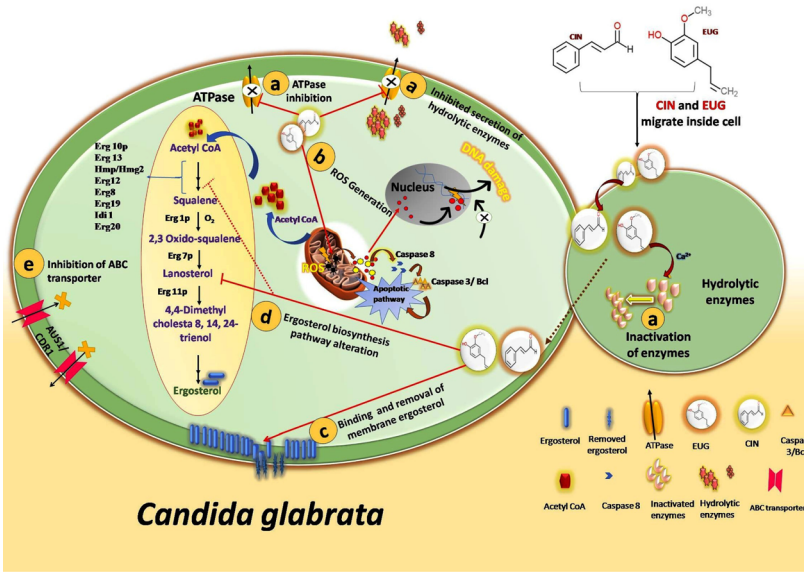

Figure 11. Schematic diagram representing possible antifungal mechanism (a–e) of CIN and EUG in *C. glabrata*. (a) By inhibition of membrane ATPase pump which mediates secretion of hydrolytic enzyme or by degradation of hydrolytic enzymes; (b) by ROS generation which results in release of cyt *c* and activates proapoptotic pathways; (c) by disturbing cell membrane integrity via removal of membrane ergosterol; (d) by inhibiting/altering the functionality of biosynthetic pathway enzymes similar to ergosterol; and (e) by blocking import of extracellular sterol or downregulating the expression of ABC sterol importer and drug transporter.

activity and molecular target of CIN in combination with citral has been elucidated against *Penicillium expansum* growth.[46] Besides this, many researchers have highlighted the potential of phytoactive molecules against bacterial and fungal species.[47−49]

In this investigation, the antifungal activity of two effective phytoactive molecules (CIN and EUG) was studied against two different growth forms (planktonic and sessile) of *C. glabrata* and its clinical isolates. The effect of CIN and EUG on *C. glabrata* cell wall, ROS generation, ECM, transcription of selected genes, and hydrophobicity was also explored and compared with that of CCG3. The results indicated *C. glabrata* biofilm eradicating potency of CIN and EUG from clinically relevant biomaterials (contact eye lens and urinary catheter). Data suggested that clinical isolate (CCG3) is more resistant, more surface adhering, and hydrophobic, as compared to *C. glabrata*, although no significant changes were observed in their ECM biochemical compositions. Similar variation in biofilm-forming ability of clinical isolates as compared to *Candida* laboratory strain has been reported by other researchers.[50,51] The plausible mechanisms observed for such a variation is the ability of pathogens to modulate their biochemical composition/differential adherence/hydrophobicity ability, which is the resultant of exposure to antifungal agents, close contact with host, and timely mutations.[20,25,51]

Molecular Insights into *C. glabrata* Biofilm Eradication Mechanism by CIN and EUG. The antimicrobial property of natural compounds or molecules depends on the functional group present in them.[52] CIN is a naturally occurring organic compound in cinnamon oil, whereas EUG is a phenylpropanoid present in aromatic plants and a major component of clove oil.[53,54] The antimicrobial activity of both compounds is due to their lipophilic nature they interact with hydrophobic components (ergosterol) of cell membrane to generate pores. This eventually reduces cell membrane integrity and permeability, thus resulting in cell lysis and leakage of intracellular contents (nucleic acid, protein, and ATP) from the cell.[46,53,55−59] CIN exposure might mediate damage to *C. glabrata* cell membrane in a similar way, as evident from results which depicts increased release of nucleic acid followed by cell death, without any change in ergosterol content (Figures 6 and 9). EUG also causes cell death as well as release of nucleic acid (Figure 6); and unlike CIN, EUG increased the cell membrane ergosterol content (Figure 9), indicating that EUG and CIN interacts differently with cell membrane ergosterol.

Previously, researchers have reported strong inhibitory effect of CIN on plasma membrane ATPase which has a potential role in the secretion of hydrolytic enzymes.[60] However, upsurge of this ATPase-dependent transportation of hydrolytic enzymes enhances secreted aspartyl proteases activity in *C. albicans*.[61] Therefore, the observed decrease in the proteinase and phospholipase activity in this study can be attributed to the de-escalation of CIN/EUG-mediated ATPase, which decreased the efflux of hydrolytic enzymes across cell membrane and ultimately results in less enzymatic activity (Figure 4D,E). In line with our observations, CIN reduced the proteinase and phospholipase activities in *C. albicans*.[62]

Many studies have also proposed that the antifungal activity of CIN is due to its inhibitory effect on cell wall and membrane synthesizing enzymes, mainly 1,3-β-glucan, chitin, and ergosterol.[63−66] It is worth noting that cells cannot overcome the stress of ergosterol deficiency and were more susceptible to stress conditions as ergosterol is a crucial ingredient of fungal cell membrane in terms of membrane rigidity, fluidity, and permeability.[29,67] CIN induced moderate transcriptional downregulation of *ERG2*, *ERG3*, *ERG4*, and *ERG11* and was in congruence with the data of ergosterol content which showed no significant changes although the ergosterol importer gene *AUS1* was significantly downregulated (Figure 9, Table 3). However, RT-PCR results of EUG-treated *C. glabrata* showed upregulation of *ERG* genes and an increase in ergosterol content. These results are in sharp contrast with the previous findings because of a drop in ergosterol content in *C. albicans* at fungicidal concentrations of EUG.[68] Moreover, in

DOI: 10.1021/acsomega.8b01856
ACS Omega 2018, 3, 12201−12214

Trichophyton rubrum, also EUG did affect ergosterol content.[69] The differences in the ergosterol content observed in the present case with respect to other studies can be attributed to: (a) the differential composition of cell membrane of *C. glabrata* to that of *C. albicans* and *T. rubrum* and (b) difference in EUG concentrations because this study used subinhibitory concentration (64 μg mL^{-1}).

CIN is also a known noncompetitive inhibitor of 1,3-β-glucan synthase and mixed inhibitor of chitin synthase in *Saccharomyces cerevisiae* and thus acts as cell-wall-active antifungal molecule.[63,69] Interestingly, a significant decrease in the expression of *FKS1* (1,3-β-glucan synthase) and *KRE1* (cell wall biogenesis) was observed in CIN/EUG-treated cells. These data are in support of previous observations suggesting the importance of using CIN and EUG as antifungal molecule against *C. glabrata*.

In addition to cell wall and membrane, CIN is also responsible for oxidative stress generation and apoptosis.[70] CIN increases the MMP that leads to ROS generation and release of cyt *c* from mitochondria to cytoplasm.[70] In *C. albicans,* CIN induces apoptosis via metacaspase-dependent pathway activated by cytochrome *c* release and ROS generation. Increased MMP is an early event of apoptosis, whereas ROS and cytochrome *c* are known to activate the proapoptotic pathway.[71] Similarly, EUG is also known to induce oxidative stress which causes lipid peroxidation of cytoplasmic membrane lipids and finally cell death.[72] Earlier researchers mentioned that EUG induces apoptosis in *C. albicans* as a consequence of the inhibition of cell cycle progression at G1−S and G2−M phases.[73] ROS, MMP, and cytochrome *c* results of CIN/EUG-exposed *C. glabrata* cells were in agreement with the prior indications of CIN/EUG-induced apoptosis. The activity of catalase enzyme, which is known to protect cell from ROS, was found to be reduced in CIN/EUG-treated *C. glabrata* biofilm cells which is in resemblance with the increased catalase activity in CIN-exposed *C. albicans*.[46] Considering these evidence, the mechanism of action through which CIN and EUG exhibit antifungal activity can be highlighted by the following cellular features (Figure 11). They include: (a) inhibition of plasma membrane ATPase which has a role in secretion of hydrolytic enzyme, (b) ROS generation and apoptosis, (c) damaging cell structure by binding and removing membrane ergosterol, (d) disturbing functionality of genes involved in membrane biosynthesis such as *ERG* genes, *FKS1* and *KRE1*, and (e) inhibiting membrane ATP binding cassette (ABC) sterol importer and drug transporter.

CONCLUDING REMARKS

The current study highlights the antibiofilm activity of phytoactive molecules (CIN and EUG) in *C. glabrata* and its clinical isolates. These two compounds are mediating the antifungal activity via deactivating its hydrolytic enzymes, ROS generation, apoptosis, and selectively modulating the ergosterol content. The study established that these compounds are highly effective in their biofilm eradication properties even on clinically relevant biomaterials such as urinary catheter and eye lens. The benefit of using phytoactive molecules in antifungal therapy is that no new formulation development is needed for their therapeutic application as they are naturally present in EOs. A recent study reported that EO components, such as CIN, EUG, thymol, and carvacrol, exhibited excellent antimicrobial activity against bacterial biofilms and shown better cytotoxicity values against fibroblasts, macrophages, and keratinocytes cell lines compared to the traditional antiseptic drug chlorhexidine.[74] Moreover, these EOs are kept under GRAS category by FDA (U.S.).[75] Indeed, CIN is an active component of cinnamon oil, which has passed clinical trial phase 1 for treatment of oral candidiasis.[76] Furthermore, EUG containing clove oil has also been widely used in dentistry for treating dental caries and periodontal diseases.[77,78] The study demonstrates that coating of medical implant devices with CIN and EUG will help in preventing implant-associated fungal infections. With these perspectives, we believe that naturally occurring phytoactive molecules stand out as a potential source of bioactive molecule with immense therapeutic applications in treating dental, oral, and superficial fungal infections.

MATERIALS AND METHODS

Strain Collection and Culturing of *C. glabrata* and Its Clinical Isolates. *C. glabrata* (CG; MTCC 3019) used in the study was procured from IMTECH (Microbial Type Culture Collection), Chandigarh, India. *C. glabrata* clinical isolates (CCG1, CCG2, CCG3, and CCG4) used in this study were a kind gift from Dr. Navin Kumar, Graphic Era Deemed to be University, Dehradun, India.[79] Clinical isolates of *C. glabrata* were classified as susceptible (CCG4), susceptible dose-dependent (CCG2), and resistant (CCG1 and CCG3) according to interpretive guidelines for in vitro susceptibility testing of *Candida* species for fluconazole.[79] All strains were routinely maintained and cultured in YPD media (1% yeast extract, 2% dextrose, and 2% peptone; 2% agar for solid media) at 37 °C. The urinary catheter and eye lens (EtafilconA; 14.0 DIA) were purchased locally. All chemicals used in the study were procured from Sigma-Aldrich chemicals Ltd and Himedia, India. RNeasy kit and RT-PCR reagents were purchased from QIAGEN and Applied Biosystems, respectively. Stock solutions of CIN and EUG were prepared in dimethyl sulfoxide.

Biofilm Formation Studies on *C. glabrata* and Its Clinical Isolates. Biofilm forming ability of *C. glabrata* and its clinical isolates were studied in 96-well flat bottom MTPs in RPMI medium (Roswell Park Memorial Institute). Log-phase cultures of all strains were diluted individually in phosphate-buffered saline (PBS) (pH 7.0) to a concentration of 1×10^7 cells mL^{-1}. The suspension (100 μL) of these cells was separately added to wells of MTP and incubated for 90 min. After incubation, PBS was replaced with RPMI, and MTP was again incubated at 37 °C. For quantification of biofilm formed at different time intervals (2, 4, 8, 10, 12, 24, and 48 h), XTT reduction assay was used.[80]

For studying the effect of CIN and EUG on *C. glabrata* and its clinical isolate biofilm, log phase cells were diluted in sterile PBS to a concentration of 1×10^7 cells mL^{-1}, and 100 μL of suspension was added into each well of MTP.[81] Plates were then incubated at 37 °C for 90 min (adhesion phase), and 200 μL of RPMI containing CIN and EUG in the concentration range of 512−2 μg mL^{-1} was added after washing wells thrice with PBS. The plates were again incubated for 48 h, and the inhibitory effect of CIN and EUG was evaluated in terms of metabolic activity by XTT reduction assay.

For mature biofilm, after 90 min incubation of adhesion phase, wells were washed with PBS and 200 μL of RPMI was added. Then, plates were reincubated for 48 h followed by washing with PBS, and 200 μL of RPMI containing CIN and EUG in the concentration range of 512−2 μg mL^{-1} was added.

DOI: 10.1021/acsomega.8b01856
ACS Omega 2018, 3, 12201−12214

The eradicating effect of CIN and EUG on biofilm was evaluated by XTT reduction assay after 24 h of incubation.

Minimum Inhibitory Concentration Measurements. The inhibitory effect of six different phytoactive molecules was initially screened against *C. glabrata* in MTP as per M27-A2 guidelines for yeast broth microdilution.[82] The concentration of log phase *C. glabrata* cells was adjusted to 2.5×10^3 cells mL^{-1} in RPMI medium. Briefly, 100 μL of cell suspension was added into each well of MTP and 100 μL of twofold diluted phytoactive molecule in RPMI media (range 1024−32 μg mL^{-1}) was also added. The plates were incubated for 48 h at 37 °C and visualized for growth in the form of turbidity. The results are represented as MIC_{90} values; a concentration where 90% growth was inhibited as compared to control.

MFC Measurements. MFC of phytoactive molecules was determined against *C. glabrata* and its clinical isolates on YPD agar media plates. The 48 h-treated cells from MTP of MIC were spotted on to solid media plates. The drop was then air dried and incubated at 37 °C for 18 h. After incubation, plates were photographed on a black background.[79]

Determination of Ergosterol Content. Ergosterol content in the cell membrane of *C. glabrata* and CCG3 cells was measured by incubating log phase cells in sabouraud dextrose broth with or without CIN (32 μg mL^{-1}) and EUG (64 μg mL^{-1}) for 24 h at 37 °C.[69] The cells were centrifuged at 6000 rpm for 5 min, and the pellet was washed with sterile water. The wet weight of the cell pellet was measured, and the pellet was suspended in 3 mL of lysing agent (25% alcoholic KOH) and vortexed for 1 min. Cell suspension was incubated for 1 h at 85 °C in water bath. Then, sterols were extracted by adding a mixture of distilled water and *n*-heptane in a 1:3 ratio, followed by vigorous vortexing. The heptane layer was collected carefully in glass tubes and stored for 24 h at −20 °C. The sterol extracts were studied by mixing 20 μL of sample and 100 μL of absolute ethanol and scanning from 230 to 300 nm using a UV−visible spectrophotometer. The amount of ergosterol was quantified by using the following equation

$$\%\ \mathrm{ERG} = \frac{\left[\left(\frac{A_{281}}{290}\right) \times F\right]}{\text{pellet weight}} - \frac{\left[\left(\frac{A_{230}}{518}\right) \times F\right]}{\text{pellet weight}} \times 100$$

where F is the dilution factor; 290 and 518 are the E values for crystalline ergosterol and 24(28) dehydroergosterol, respectively.

ROS Generation. ROS level in *C. glabrata* and CCG3 biofilm cells on exposure to lethal concn of CIN (128 μg mL^{-1}) and EUG (256 μg mL^{-1}) was studied by adding a mixture of DCFDA (10 μM) and propidium iodide (1 mg mL^{-1} PI) in MTP, as described earlier.[83] The MTP was incubated in dark for 30 min at 37 °C. For measurement of ROS generation in biofilm cells, DCFDA fluorescence was recorded at an emission wavelength of 520 nm and excitation wavelength of 485 nm. Whereas the emission and excitation wavelength for PI was taken at 617 and 543 nm, respectively. Fluorescence microscopic images of cells were taken at 40× magnification in fluorescence microscope.

Biochemical Composition of ECM. ECM was isolated from *C. glabrata* and CCG3 biofilm developed in the presence of CIN and EUG by scrapping it from the MTP well surface using sterile scrapper and sterile PBS (pH 7.0). The scrapped biofilm was sonicated (Q700 sonicator, QSonica) at 35 W in an ice bath for five cycles of 30 s each, as described by Fonseca et al.[84] The suspension was centrifuged at 12 000 rpm for 5 min. The supernatant was then used for biochemical and enzymatic analysis of ECM, whereas the cell pellet was used for catalase activity measurement. The ECM was examined for carbohydrate, protein, and eDNA quantification. Phenol−sulfuric acid method was used for total carbohydrate estimation with glucose as a standard. Briefly, 1 mL of H_2SO_4, 200 μL of phenol (5% w/v), and 100 μL of sample were mixed in glass tubes. The tubes were then incubated at 30 °C for 30 min. Then, tubes were cooled and the absorbance was measured at 485 nm. For total protein measurement, BCA kit was used with bovine serum albumin (BSA) as a standard. The absorbance was measured at 562 nm. The quantity of eDNA in sample was measured by precipitating the eDNA. Precipitation was done by adding one-tenth the volume of sodium acetate (3 M) in a sample, followed by adding phenol, chloroform, and isoamyl alcohol (25:24:1). The aqueous layer was collected in fresh tube, and 2.5 volume of ethanol was added to precipitate the eDNA. The purity of eDNA was checked by using nanodrop by 260/280 ratio.

Phospholipase and Proteinase Activity. At neutral pH, the activity was measured by preparing the substrate consisting of 50 mM Tris-HCl buffer (pH 7.5), 1.6 mM phosphatidylcholine (min. 41%), 0.25% Triton X-100, 20 mM $AlCl_3$, and 0.124% bromothymol blue. The solution was then filtered and stored at 4 °C. Before absorbance was measured, the pH of ECM was adjusted to 7.5 with 10 mM NaOH. The phospholipasic activities were determined by mixing 100 μL of ECM with 900 μL of substrate and the reading was taken at OD_{630} nm. The specific phospholipase activity was recorded as the absorbance shift per minute of the reaction. The proteinase activity was determined by mixing 1% w/v azocasein substrate with the supernatants and incubating it at 37 °C for 1 h. Trichloroacetic acid (10%) was used to stop the reaction, and the mixture was centrifuged for 5 min at 12 000 rpm. The supernatant obtained was then mixed with 0.5 M NaOH and incubated for 15 min. The proteinase activity was measured at 440 nm. The specific proteinase activity was the amount of enzyme that elicited an increase of 0.001 units in absorbance per minute of reaction.[83]

Catalase Activity. The catalase activity of CIN- and EUG-treated *C. glabrata* and CCG3 sessile cells collected after ECM isolation were lysed with glass beads.[85] The samples were then centrifuged at 10 000 rpm, and the supernatant was collected. For determining the catalase activity, 333 μL of 50 mM H_2O_2, 567 μL of PBS (pH 7.0), and 100 μL of supernatant were mixed, followed by measuring absorbance of sample at 240 nm. One unit of catalase activity corresponded to the amount of enzyme that decomposes 1 μmol of H_2O_2 per minute of reaction at 37 °C. The catalase activity (U/mg) was calculated using the following formula

$$\frac{\mathrm{U}}{\mathrm{mg}} = \frac{(A_0 - A_2) \times V_t}{\sum_{240} \times d \times V_s \times C_t \times 0.001}$$

where, $A_0 - A_2$ is the difference in absorbance; V_t is the total volume of reaction; V_s is the volume of sample; Σ_{240} is the molar extinction coefficient for H_2O_2; d is the optical path length of cuvette; and C_t is the protein concentration in sample.

Hydrophobicity Assay. To determine hydrophobicity, overnight grown *C. glabrata* and CCG3 cell at 0.1 OD_{600} were exposed to subinhibitory concentration of CIN (64 μg mL^{-1}) and EUG (128 μg mL^{-1}) and then incubated for 24 h at 37 °C.

DOI: 10.1021/acsomega.8b01856
ACS Omega 2018, 3, 12201−12214

Cells were harvested after incubation, washed with sterile PBS, and suspended in 3 mL of 50 mM sodium phosphate buffer (pH 7.2) at a concentration of 2×10^6 cells mL^{-1}. Octane (500 μL) was then added to cell suspension and vortexed for 1 min. Cells present in aqueous phase were calculated by taking absorbance at OD_{600}.[86] The HI was calculated by the following equation

$$HI = \frac{A_1 - A_2}{A_1} \times 100\%$$

where A_1 is the absorbance of inoculum and A_2 is the absorbance of aqueous phase.

Cytochrome *c* Determination. Briefly, early stationary phase cells were diluted in PBS to a concentration of 1×10^7 cells mL^{-1} and further incubated in 3 mL of YPD broth containing CIN (128 μg mL^{-1}) and EUG (256 μg mL^{-1}) separately at 30 °C for 24 h. The cells were washed with PBS, and the pellet was suspended in the homogenization medium [50 mM Tris (pH 7.5) 2 mM EDTA, 2% glucose, and 1 mM phenylmethylsulfonyl fluoride]. The suspension was vortexed and centrifuged at 5000 rpm for 10 min. The supernatant so obtained was again centrifuged at 20 000 rpm for 45 min. After centrifugation, the supernatant was quantified for cyt *c* released from mitochondria to cytoplasm. Whereas the pellet was suspended in 50 mM Tris (pH 5.0) having 2 mM EDTA and incubated for 5 min at 37 °C. The dissolved pellet again centrifuged at 10 000 rpm for 30 s was used for the determination of cyt *c* remaining in mitochondria. Protein content in the supernatant and the pellet was estimated by Bradford reagent kit, using BSA as the standard. Before quantifying cyt *c* quantity in supernatant and pellet, both were reduced with 500 mg L^{-1} ascorbic acid at room temperature for 5 min, and the absorbance was measured at 550 nm.[70]

Mitochondrial Membrane Potential. For studying the change in MMP, log phase *C. glabrata* cells were incubated in SDB medium with or without CIN and EUG for 6 h at 37 °C in shaking. After incubation, cells were collected by centrifugation and washed with PBS (pH 7.0). Then, cells were suspended in 10 mM HEPES buffer (pH 7.4) containing 5% glucose and 100 nM rhodamine B. The suspension was incubated for 30 min in dark at 37 °C. After incubation, cells were washed and MMP was visualized by fluorescence microscope at the excitation wavelength of 555 nm and emission wavelength of 579 nm.[87]

FESEM Measurements. FESEM was used to monitor the morphological changes in *C. glabrata* and CCG3 (resistant isolate) biofilm cells before and after treatment with CIN and EUG. Briefly, 1 cm^2 polystyrene discs were incubated in fetal calf serum for 24 h. After incubation, polystyrene discs were placed in 24-well plates, and 1 mL of cell suspension prepared in RPMI medium was added. Plates were incubated for 48 h, and then medium was replaced with CIN- and EUG-containing media. Plates were again incubated for 24 h after which discs were washed with PBS and fixed overnight in 2.5% gluteraldehyde solution. Discs were then again washed with PBS and treated with ethanol gradient. Air dried samples were mounted on stubs, and gold sputtering was done. Finally, samples were visualized under FESEM at a voltage of 15 kV and magnification from 1000 to 5000×.[88]

Release of Nucleic Acid Content. The rate of release of nucleic acid from *C. glabrata* and CCG3 cells exposed to CIN (128 μg mL^{-1}) and EUG (256 μg mL^{-1}) for 2, 4, and 8 h at 37 °C was measured by taking absorbance at 260 nm.[89] Cells exposed to alcoholic KOH which causes 100% cellular leakage were used as a reference sample. The sample was centrifuged at 5000 rpm for 5 min, and the supernatant collected was used for measuring the intracellular leakage in terms of rate of release of DNA from *C. glabrata* and CCG3 cells.

Fluorescence Microscopy Studies. For studying the effect of CIN and EUG on the biofilm cell viability, biofilm of *C. glabrata* and CCG3 developed was washed with PBS (pH 7.0) after CIN and EUG treatment. Then, biofilm was stained with FDA (2 μg mL^{-1} fluorescein diacetate) and PI (0.6 μg mL^{-1} propidium iodide).[90] Plate was incubated for 20 min at room temperature in dark, and wells were washed before visualization under fluorescence microscope. All images were captured at 40× magnification.

Transcriptional Analysis. Effect of CIN (32 μg mL^{-1}) and EUG (64 μg mL^{-1}) subinhibitory concentration on the expression of selected *C. glabrata* and CCG3 was studied by qRT-PCR. Log-phase cells were treated with CIN and EUG in YPD broth. Total RNA was extracted from cells by using RNeasy kit, QIAGEN by following manufacturer's instructions. The RNA was quantified by a nanodrop (Thermo Fisher Scientific), which was used for cDNA synthesis using Verso cDNA synthesis kit, Thermo. Primers for RT-PCR of the above-mentioned genes and housekeeping gene (*ACT1*) were designed by using Primer Quest, Integrated DNA Technologies (IDT) and were synthesized by IDT (Table 3). SYBR green mix (Applied Biosystems) was used in Mastercycler for qRT-PCR. cDNA template (100 ng) and gene-specific forward and reverse primers (200 nM) were used in the reaction. The following parameters were used for qRT-PCR: an initial denaturation at 95 °C (3 min), followed by 40 cycles of denaturation (95 °C/30 s), annealing (52 °C/30 s), and extension (72 °C/30 s), melting-curve analysis starting from initial temperature 45 to 95 °C, with a gradual increase in 0.5 °C/15 s. Specificity of the primers was confirmed by the melting curve analysis. The generated CT values of target genes were normalized to the CT value of housekeeping *ACT1* gene. Relative expression fold changes were evaluated by ΔΔCT method using $2^{-\Delta\Delta CT}$ formula.[91]

Biofilm Study on Biomaterials. Commercially available urinary catheter (silicone) and contact eye lens were procured from a local medical store and were used as biomaterials for biofilm study. Contact lens were used as a whole, whereas 1 cm long pieces of urinary catheter coupons were cut out and sterilized with 100% ethylene oxide and kept under UV for 4 h.[92−94] Sterile lens and catheter coupons were incubated in RPMI medium containing 1×10^7 cells mL^{-1} for 48 h. Biomaterials with biofilms were treated for 24 h with CIN and EUG containing RPMI and then was quantified by XTT reduction assay.

Statistical Analysis. All experiments were performed in triplicates, and the values presented the mean with standard deviation, obtained from three different observations for each assay. Student's *t*-test was used for the statistical analysis, and a value of $P < 0.05$ was considered statistically significant (*), $P < 0.01$ as highly significant (**) and $P < 0.001$ as extremely significant (***).

.

DOI: 10.1021/acsomega.8b01856
ACS Omega 2018, 3, 12201−12214

■ ASSOCIATED CONTENT

Supporting Information

The Supporting Information is available free of charge on the ACS Publications website at DOI: 10.1021/acsomega.8b01856.

Candida glabrata biofilm inhibition, mature biofilm eradication, cell hydrophobicity, primer sequence, and metabolic activity of *C. glabrata* biofilm on urinary catheter and contact eye lens (PDF)

■ AUTHOR INFORMATION

Corresponding Authors

*E-mail: vikasfbs@iitr.ac.in, vikasfbs@gmail.com. Phone: 091-1332-285530. Fax: 091-1332-273560 (V.P.).

*E-mail: mohanpmk@gmail.com, krishfbt@iitr.ac.in. Phone: 091-1332-284779 (K.M.P.).

ORCID

Krishna Mohan Poluri: 0000-0003-3801-7134

Author Contributions

P.G., V.P., and K.M.P. participated in the study design and preparation of the manuscript. P.G. and N.K. procured the clinical isolates of *C. glabrata* and performed the experiments. P.G., S.G., and M.S. analyzed the data. All authors have read and approved the final version of the manuscript.

Notes

The authors declare no competing financial interest.

■ ACKNOWLEDGMENTS

P.G. acknowledges the financial support of NPDF Grant PDF/2016/001670, from Science and Engineering Research Board (SERB), Government of India. K.M.P. acknowledges the receipt of DBT-IYBA fellowship and SERB-LS young scientist award. Authors are thankful to the Institute Instrumentation Centre, IIT Roorkee, for the microscopy analysis. Authors are grateful to Dr. V. K. Kateria, Department of Microbiology, Shri Guru Ram Rai Institute of Medical and Health Sciences, Dehradun, for the clinical isolates of *C. glabrata*.

■ REFERENCES

(1) Dadar, M.; Tiwari, R.; Karthik, K.; Chakraborty, S.; Shahali, Y.; Dhama, K. Candida Albicans-Biology, Molecular Characterization, Pathogenicity, and Advances in Diagnosis and Control−An Update. *Microb. Pathog.* **2018**, *117*, 128−138.

(2) Healey, K. R.; Nagasaki, Y.; Zimmerman, M.; Kordalewska, M.; Park, S.; Zhao, Y.; Perlin, D. S. The Gastrointestinal Tract Is a Major Source of Echinocandin Drug Resistance in a Murine Model of Candida Glabrata Colonization and Systemic Dissemination. *Antimicrob. Agents Chemother.* **2017**, *61*, No. e01412-17.

(3) Morgan, J. Global Trends in Candidemia: Review of Reports from 1995−2005. *Curr. Infect. Dis. Rep.* **2005**, *7*, 429−439.

(4) Pfaller, M. A.; Diekema, D. J. Epidemiology of Invasive Candidiasis: A Persistent Public Health Problem. *Clin. Microbiol. Rev.* **2007**, *20*, 133−163.

(5) Yapar, N. Epidemiology and Risk Factors for Invasive Candidiasis. *Ther. Clin. Risk Manage.* **2014**, *10*, 95.

(6) Mushi, M. F.; Mtemisika, C. I.; Bader, O.; Bii, C.; Mirambo, M. M.; Groß, U.; Mshana, S. E. International Journal of Infectious Diseases High Oral Carriage of Non- albicans Candida Spp. among HIV-Infected Individuals. *Int. J. Infect. Dis.* **2016**, *49*, 185−188.

(7) Chapman, B.; Slavin, M.; Marriott, D.; Halliday, C.; Kidd, S.; Arthur, I.; Bak, N.; Heath, C. H.; Kennedy, K.; Morrissey, C. O. Changing Epidemiology of Candidaemia in Australia. *J. Antimicrob. Chemother.* **2017**, *72*, 1103−1108.

(8) Lamoth, F.; Lockhart, S. R.; Berkow, E. L.; Calandra, T. Changes in the Epidemiological Landscape of Invasive Candidiasis. *J. Antimicrob. Chemother.* **2018**, *73*, i4−i13.

(9) Bhattacharjee, P. Epidemiology and Antifungal Susceptibility of Candida Species in a Tertiary Care Hospital, Kolkata, India. *Curr. Med. Mycol.* **2016**, *2*, 20.

(10) Sharma, Y.; Chumber, S.; Kaur, M. Studying the Prevalence, Species Distribution, and Detection of in Vitro Production of Phospholipase from Candida Isolated from Cases of Invasive Candidiasis. *J. Global Infect. Dis.* **2017**, *9*, 8.

(11) Gandhi, V.; Patel, M. Prevalence of Candida Species and Its Antifungal Susceptibility Isolated from Blood Culture at Tertiary Care Hospital, Ahmedabad, India. *Int. J. Curr. Microbiol. Appl. Sci.* **2017**, *6*, 884−892.

(12) Kalaiarasan, K.; Singh, R.; Chaturvedula, L. Fungal Profile of Vulvovaginal Candidiasis in a Tertiary Care Hospital. *J. Clin. Diagn. Res.* **2017**, *11*, DC06.

(13) Sadeghi, G.; Ebrahimi-Rad, M.; Mousavi, S. F.; Shams-Ghahfarokhi, M.; Razzaghi-Abyaneh, M. Emergence of Non-Candida Albicans Species: Epidemiology, Phylogeny and Fluconazole Susceptibility Profile. *J. Mycol. Med.* **2018**, *28*, 51−58.

(14) Goswami, D.; Goswami, R.; Banerjee, U.; Dadhwal, V.; Miglani, S.; Lattif, A. A.; Kochupillai, N. Pattern of Candida Species Isolated from Patients with Diabetes Mellitus and Vulvovaginal Candidiasis and Their Response to Single Dose Oral Fluconazole Therapy. *J. Infect.* **2006**, *52*, 111−117.

(15) Ray, D.; Goswami, R.; Banerjee, U.; Dadhwal, V.; Goswami, D.; Mandal, P.; Sreenivas, V.; Kochupillai, N. Prevalence of Candida Glabrata and Its Response to Boric Acid Vaginal Suppositories in Comparison with Oral Fluconazole in Patients with Diabetes and Vulvovaginal Candidiasis. *Diabetes Care* **2007**, *30*, 312−317.

(16) Hachem, R.; Hanna, H.; Kontoyiannis, D.; Jiang, Y.; Raad, I. The Changing Epidemiology of Invasive Candidiasis. *Cancer* **2008**, *112*, 2493−2499.

(17) Silva, S.; Hooper, S. J.; Henriques, M.; Oliveira, R.; Azeredo, J.; Williams, D. W. The Role of Secreted Aspartyl Proteinases in Candida Tropicalis Invasion and Damage of Oral Mucosa. *Clin. Microbiol. Infect.* **2011**, *17*, 264−272.

(18) Whaley, S. G.; Berkow, E. L.; Rybak, J. M.; Nishimoto, A. T.; Barker, K. S.; Rogers, P. D. Azole Antifungal Resistance in Candida Albicans and Emerging Non-Albicans Candida Species. *Front. Microbiol.* **2017**, *7*, 2173.

(19) Cavalheiro, M.; Teixeira, M. C. Candida Biofilms: Threats, Challenges, and Promising Strategies. *Front. Med.* **2018**, *5*, 28.

(20) Vitali, A.; Vavala, E.; Marzano, V.; Leone, C.; Castagnola, M.; Iavarone, F.; Angiolella, L. Cell Wall Composition and Biofilm Formation of Azoles-Susceptible and-Resistant Candida Glabrata Strains. *J. Chemother.* **2017**, *29*, 164−172.

(21) Pierce, C.; Vila, T.; Romo, J.; Montelongo-Jauregui, D.; Wall, G.; Ramasubramanian, A.; Lopez-Ribot, J. The Candida Albicans Biofilm Matrix: Composition, Structure and Function. *J. Fungi* **2017**, *3*, 14.

(22) Panariello, B. H. D.; Klein, M. I.; Mima, E. G. D. O.; Pavarina, A. C. Fluconazole Impacts the Extracellular Matrix of Fluconazole-Susceptible and-Resistant Candida Albicans and Candida Glabrata Biofilms. *J. Oral Microbiol.* **2018**, *10*, 1476644.

(23) Mitchell, K. F.; Zarnowski, R.; Andes, D. R. Fungal Super Glue: The Biofilm Matrix and Its Composition, Assembly, and Functions. *PLoS Pathog.* **2016**, *12*, No. e1005828.

(24) Martins, M.; Henriques, M.; Lopez-Ribot, J. L.; Oliveira, R. Addition of DNase Improves the in Vitro Activity of Antifungal Drugs against Candida Albicans Biofilms. *Mycoses* **2012**, *55*, 80−85.

(25) Dabiri, S.; Shams-Ghahfarokhi, M.; Razzaghi-Abyaneh, M. Comparative Analysis of Proteinase, Phospholipase, Hydrophobicity and Biofilm Forming Ability in Candida Species Isolated from Clinical Specimens. *J. Mycol. Med.* **2018**, *28*, 437−442.

(26) Kong, E. F.; Tsui, C.; Kucharíková, S.; Van Dijck, P.; Jabra-Rizk, M. A. Modulation of Staphylococcus Aureus Response to

DOI: 10.1021/acsomega.8b01856
ACS Omega 2018, 3, 12201−12214

Antimicrobials by the Candida Albicans Quorum Sensing Molecule Farnesol. *Antimicrob. Agents Chemother.* **2017**, *61*, No. e01573-17.
(27) Dupont, S.; Lemetais, G.; Ferreira, T.; Cayot, P.; Gervais, P.; Beney, L. Ergosterol Biosynthesis: A Fungal Pathway for Life on Land? *Evolution Int. J. Org. Evolution* **2012**, *66*, 2961−2968.
(28) Stylianou, M.; Kulesskiy, E.; Lopes, J. P.; Granlund, M.; Wennerberg, K.; Urban, C. F. Antifungal Application of Non-Antifungal Drugs. *Antimicrob. Agents Chemother.* **2013**, *58*, 1055.
(29) Li, Q.; Tsai, H.-F.; Mandal, A.; Walker, B.; Noble, J.; Fukuda, Y.; Bennett, J. Sterol Uptake and Sterol Biosynthesis Act Coordinately to Mediate Antifungal Resistance in Candida Glabrata under Azole and Hypoxic Stress. *Mol. Med. Rep.* **2018**, *17*, 6585−6597.
(30) Bordallo-Cardona, M. Á.; Marcos-Zambrano, L. J.; Sánchez-Carrillo, C.; de la Pedrosa, E. G. G.; Cantón, R.; Bouza, E.; Escribano, P.; Guinea, J. Mutant Prevention Concentration and Mutant Selection Window of Micafungin and Anidulafungin in Clinical Candida Glabrata Isolates. *Antimicrob. Agents Chemother.* **2018**, *62*, No. e01982-17.
(31) Roemer, T.; Krysan, D. J. Antifungal Drug Development: Challenges, Unmet Clinical Needs, and New Approaches. *Cold Spring Harbor Perspect. Med.* **2014**, *4*, a019703.
(32) Brackman, G.; Coenye, T. Quorum Sensing Inhibitors as Anti-Biofilm Agents. *Curr. Pharm. Des.* **2015**, *21*, 5−11.
(33) Tang, K.; Zhang, X.-H. Quorum Quenching Agents: Resources for Antivirulence Therapy. *Mar. Drugs* **2014**, *12*, 3245−3282.
(34) Abraham, W.-R. Going beyond the Control of Quorum-Sensing to Combat Biofilm Infections. *Antibiotics* **2016**, *5*, 3.
(35) Koh, C.; Sam, C.; Yin, W.; Tan, L. Y.; Krishnan, T.; Chong, Y. M.; Chan, K. Plant-Derived Natural Products as Sources of Anti-Quorum Sensing Compounds. *Sensors* **2013**, *13*, 6217−6228.
(36) Srivastava, A.; Singh, B. N.; Deepak, D.; Rawat, A. K. S.; Singh, B. R. Colostrum Hexasaccharide, a Novel Staphylococcus Aureus Quorum- Sensing Inhibitor. *Antimicrob. Agents Chemother.* **2015**, *59*, 2169−2178.
(37) Fetzner, S. Quorum Quenching Enzymes. *J. Biotechnol.* **2015**, *201*, 2−14.
(38) Lade, H.; Paul, D.; Kweon, J. H. Quorum Quenching Mediated Approaches for Control of Membrane Biofouling. *Int. J. Biol. Sci.* **2014**, *10*, 550−565.
(39) Guleria, S.; Tiku, A. K.; Koul, A.; Gupta, S.; Singh, G.; Razdan, V. K. Antioxidant and Antimicrobial Properties of the Essential Oil and Extracts of Zanthoxylum Alatum Grown in North-Western Himalaya. *Sci. World J.* **2013**, *2013*, 1−9.
(40) Ahmad, A.; Khan, A.; Khan, L. A.; Manzoor, N. Vitro Synergy of Eugenol and Methyleugenol with Fluconazole against Clinical Candida Isolates. *J. Med. Microbiol.* **2010**, *59*, 1178−1184.
(41) Bacha, K.; Tariku, Y.; Gebreyesus, F.; Zerihun, S.; Mohammed, A.; Weiland-Bräuer, N.; Schmitz, R. A.; Mulat, M. Antimicrobial and Anti-Quorum Sensing Activities of Selected Medicinal Plants of Ethiopia: Implication for Development of Potent Antimicrobial Agents. *BMC Microbiol.* **2016**, *16*, 139.
(42) Brunke, S.; Hube, B. Two Unlike Cousins: Candida Albicans and C. Glabrata Infection Strategies. *Cell. Microbiol.* **2013**, *15*, 701−708.
(43) Newman, D. J.; Cragg, G. M. Natural Products as Sources of New Drugs from 1981 to 2014. *J. Nat. Prod.* **2016**, *79*, 629−661.
(44) McCall, A.; Edgerton, M. Real-Time Approach to Flow Cell Imaging of *Candida Albicans* Biofilm Development. *J. Fungi* **2017**, *3*, 13.
(45) Santos, G. C. d O.; Vasconcelos, C. C.; Lopes, A. J. O.; Cartagenes, M. D. S. D. S.; Filho, A. K. D. B.; do Nascimento, F. R. F.; Ramos, R. M.; Pires, E. R. R. B.; de Andrade, M. S.; Rocha, F. M. G. Candida Infections and Therapeutic Strategies: Mechanisms of Action for Traditional and Alternative Agents. *Front. Microbiol.* **2018**, *9*, 1351.
(46) Wang, Y.; Feng, K.; Yang, H.; Zhang, Z.; Yuan, Y.; Yue, T. Effect of Cinnamaldehyde and Citral Combination on Transcriptional Profile, Growth, Oxidative Damage and Patulin Biosynthesis of Penicillium Expansum. *Front. Microbiol.* **2018**, *9*, 597.
(47) Gupta, P.; Gautam, P.; Rai, N.; Kumar, N. An Emerging Hope to Combat Candida Albicans: Plant Based Therapeutics. *Biotechnol. Int.* **2012**, *5*, 85−114.
(48) Bacha, K.; Tariku, Y.; Gebreyesus, F.; Zerihun, S.; Mohammed, A.; Weiland-Bräuer, N.; Schmitz, R. A.; Mulat, M. Antimicrobial and Anti-Quorum Sensing Activities of Selected Medicinal Plants of Ethiopia: Implication for Development of Potent Antimicrobial Agents. *BMC Microbiol.* **2016**, *16*, 139.
(49) Alalwan, H.; Rajendran, R.; Lappin, D. F.; Combet, E.; Shahzad, M.; Robertson, D.; Nile, C. J.; Williams, C.; Ramage, G. The Anti-Adhesive Effect of Curcumin on Candida Albicans Biofilms on Denture Materials. *Front. Microbiol.* **2017**, *8*, 659.
(50) Amanloo, S.; Shams-Ghahfarokhi, M.; Ghahri, M.; Razzaghi-Abyaneh, M. Drug Susceptibility Profile of Candida Glabrata Clinical Isolates from Iran and Genetic Resistant Mechanisms to Caspofungin. *Rev. Iberoam. Micol.* **2018**, *35*, 88−91.
(51) Alnuaimi, A. D.; O'Brien-Simpson, N. M.; Reynolds, E. C.; McCullough, M. J. Clinical Isolates and Laboratory Reference Candida Species and Strains Have Varying Abilities to Form Biofilms. *FEMS Yeast Res.* **2013**, *13*, 689−699.
(52) Dorman, H. J. D.; Deans, S. G. Antimicrobial Agents from Plants: Antibacterial Activity of Plant Volatile Oils. *J. Appl. Microbiol.* **2000**, *88*, 308−316.
(53) Abdelwahab, S. I.; Mariod, A. A.; Taha, M. M. E.; Zaman, F. Q.; Abdelmageed, A. H. A.; Khamis, S.; Sivasothy, Y.; Awang, K. Chemical Composition and Antioxidant Properties of the Essential Oil of Cinnamomum Altissimum Kosterm. (Lauraceae). *Arabian J. Chem.* **2017**, *10*, 131−135.
(54) Marchese, A.; Barbieri, R.; Coppo, E.; Orhan, I. E.; Daglia, M.; Nabavi, S. F.; Izadi, M.; Abdollahi, M.; Nabavi, S. M.; Ajami, M. Antimicrobial Activity of Eugenol and Essential Oils Containing Eugenol: A Mechanistic Viewpoint. *Crit. Rev. Microbiol.* **2017**, *43*, 668−689.
(55) Pinto, E.; Vale-Silva, L.; Cavaleiro, C.; Salgueiro, L. Antifungal Activity of the Clove Essential Oil from Syzygium Aromaticum on Candida, Aspergillus and Dermatophyte Species. *J. Med. Microbiol.* **2009**, *58*, 1454−1462.
(56) Latifah-Munirah, B.; Himratul-Aznita, W. H.; Zain, N. M. Eugenol, an Essential Oil of Clove, Causes Disruption to the Cell Wall of Candida Albicans (ATCC 14053). *Front. Life Sci.* **2015**, *8*, 231.
(57) Devi, K. P.; Nisha, S. A.; Sakthivel, R.; Pandian, S. K. Eugenol (an Essential Oil of Clove) Acts as an Antibacterial Agent against Salmonella Typhi by Disrupting the Cellular Membrane. *J. Ethnopharmacol.* **2010**, *130*, 107−115.
(58) de Souza, E. L.; Almeida, E. T. d. C.; Guedes, J. P. d. S. The Potential of the Incorporation of Essential Oils and Their Individual Constituents to Improve Microbial Safety in Juices: A Review. *Compr. Rev. Food Sci. Food Saf.* **2016**, *15*, 753−772.
(59) Tsuchiya, H.; Sato, M.; Miyazaki, T.; Fujiwara, S.; Tanigaki, S.; Ohyama, M.; Tanaka, T.; Iinuma, M. Comparative Study on the Antibacterial Activity of Phytochemical Flavanones against Methicillin-Resistant Staphylococcus Aureus. *J. Ethnopharmacol.* **1996**, *50*, 27−34.
(60) Shreaz, S.; Sheikh, R. A.; Bhatia, R.; Neelofar, K.; Imran, S.; Hashmi, A. A.; Manzoor, N.; Basir, S. F.; Khan, L. A. Antifungal Activity of α-Methyl Trans Cinnamaldehyde, Its Ligand and Metal Complexes: Promising Growth and Ergosterol Inhibitors. *BioMetals* **2011**, *24*, 923−933.
(61) Wu, T.; Wright, K.; Hurst, S. F.; Morrison, C. J. Enhanced Extracellular Production of Aspartyl Proteinase, a Virulence Factor, by Candida Albicans Isolates Following Growth in Subinhibitory Concentrations of Fluconazole. *Antimicrob. Agents Chemother.* **2000**, *44*, 1200−1208.
(62) Pootong, A.; Norrapong, B.; Cowawintaweewat, S. Antifungal Activity of Cinnamaldehyde against Candida Albicans. *Southeast Asian J. Trop. Med. Public Health* **2017**, *48*, 150−158.
(63) Bang, K.-H.; Lee, D.-W.; Park, H.-M.; Rhee, Y.-H. Inhibition of Fungal Cell Wall Synthesizing Enzymes by Trans-Cinnamaldehyde. *Biosci., Biotechnol., Biochem.* **2000**, *64*, 1061−1063.

DOI: 10.1021/acsomega.8b01856
ACS Omega 2018, 3, 12201−12214

(64) Yen, T.-B.; Chang, S.-T. Synergistic Effects of Cinnamaldehyde in Combination with Eugenol against Wood Decay Fungi. *Bioresour. Technol.* **2008**, *99*, 232−236.
(65) Thakre, A. D.; Mulange, S. V.; Kodgire, S. S.; Zore, G. B.; Karuppayil, S. M. Effects of Cinnamaldehyde, Ocimene, Camphene, Curcumin and Farnesene on Candida Albicans. *Adv. Microbiol.* **2016**, *06*, 627−643.
(66) Khan, M. S.; Ahmad, I.; Cameotra, S. Phenyl Aldehyde and Propanoids Exert Multiple Sites of Action towards Cell Membrane and Cell Wall Targeting Ergosterol in Candida Albicans. *AMB Express* **2013**, *3*, 54.
(67) Parks, L. W.; Casey, W. M. Physiological Implications of Sterol Biosynthesis in Yeast. *Annu. Rev. Microbiol.* **1995**, *49*, 95−116.
(68) de Paula, S. B.; Bartelli, T. F.; Di Raimo, V.; Santos, J. P.; Morey, A. T.; Bosini, M. A.; Nakamura, C. V.; Yamauchi, L. M.; Yamada-Ogatta, S. F. Effect of Eugenol on Cell Surface Hydrophobicity, Adhesion, and Biofilm of Candida Tropicalis and Candida Dubliniensis Isolated from Oral Cavity of HIV-Infected Patients. *J. Evidence-Based Complementary Altern. Med.* **2014**, *2014*, 1−8.
(69) Pereira, F. d. O.; Mendes, J. M.; Lima, E. d. O. Investigation on Mechanism of Antifungal Activity of Eugenol against Trichophyton rubrum. *Med. Mycol.* **2013**, *51*, 507−513.
(70) Khan, S. N.; Khan, S.; Iqbal, J.; Khan, R.; Khan, A. U. Enhanced Killing and Antibiofilm Activity of Encapsulated Cinnamaldehyde against Candida Albicans. *Front. Microbiol.* **2017**, *8*, 1641.
(71) Shreaz, S.; Bhatia, R.; Khan, N.; Muralidhar, S.; Manzoor, N.; Khan, L. A. Influences of Cinnamic Aldehydes on H+ Extrusion Activity and Ultrastructure of Candida. *J. Med. Microbiol.* **2013**, *62*, 232−240.
(72) Khan, A.; Ahmad, A.; Akhtar, F.; Yousuf, S.; Xess, I.; Khan, L. A.; Manzoor, N. Induction of Oxidative Stress as a Possible Mechanism of the Antifungal Action of Three Phenylpropanoids. *FEMS Yeast Res.* **2011**, *11*, 114−122.
(73) Cao, Y.; Huang, S.; Dai, B.; Zhu, Z.; Lu, H.; Dong, L.; Cao, Y.; Wang, Y.; Gao, P.; Chai, Y.; Jiang, Y. Candidaalbicans Cells Lacking CaMCA1-Encoded Metacaspase Show Resistance to Oxidative Stress-Induced Death and Change in Energy Metabolism. *Fungal Genet. Biol.* **2009**, *46*, 183−189.
(74) García-Salinas, S.; Elizondo-Castillo, H.; Arruebo, M.; Mendoza, G.; Irusta, S. Evaluation of the Antimicrobial Activity and Cytotoxicity of Different Components of Natural Origin Present in Essential Oils. *Molecules* **2018**, *23*, 1399.
(75) Hyldgaard, M.; Mygind, T.; Meyer, R. L. Essential Oils in Food Preservation: Mode of Action, Synergies, and Interactions with Food Matrix Components. *Front. Microbiol.* **2012**, *3*, 12.
(76) Ranasinghe, P.; Pigera, S.; Premakumara, G. A. S.; Galappaththy, P.; Constantine, G. R.; Katulanda, P. Medicinal Properties of "true" Cinnamon (Cinnamomum Zeylanicum): A Systematic Review. *BMC Complementary Altern. Med.* **2013**, *13*, 275.
(77) Tanomaru-Filho, M.; Tanomaru, J. M. G.; Barros, D. B.; Watanabe, E.; Ito, I. Y. In Vitro Antimicrobial Activity of Endodontic Sealers, MTA-Based Cements and Portland Cement. *J. Oral Sci.* **2007**, *49*, 41−45.
(78) Elaissi, A.; Rouis, Z.; Salem, N. A. B.; Mabrouk, S.; ben Salem, Y.; Salah, K. B. H.; Aouni, M.; Farhat, F.; Chemli, R.; Harzallah-Skhiri, F. Chemical Composition of 8 Eucalyptus Species' Essential Oils and the Evaluation of Their Antibacterial, Antifungal and Antiviral Activities. *BMC Complementary Altern. Med.* **2012**, *12*, 81.
(79) Gupta, P.; Chanda, R.; Rai, N.; Kataria, V. K.; Kumar, N. Antihypertensive, Amlodipine Besilate Inhibits Growth and Biofilm of Human Fungal Pathogen Candida. *Assay Drug Dev. Technol.* **2016**, *14*, 291−297.
(80) Gupta, P.; Nath, S.; Meena, R. C.; Kumar, N. Comparative Effects of Hypoxia and Hypoxia Mimetic Cobalt Chloride on in Vitro Adhesion, Biofilm Formation and Susceptibility to Amphotericin B of Candida Glabrata. *Journal Med. Mycol.* **2014**, *24*, e169−e177.
(81) Gupta, P.; Meena, R. C.; Kumar, N. Functional Analysis of Selected Deletion Mutants in Candida Glabrata under Hypoxia. *3 Biotech* **2017**, *7*, 193.
(82) Rex, J. H. *Reference Method for Broth Dilution Antifungal Susceptibility Testing of Filamentous Fungi; Approved Standard, 2nd ed.*; CLSI: Wayne, PA, USA, 2008.
(83) Pemmaraju, S. C.; Padmapriya, K.; Pruthi, P. A.; Prasad, R.; Pruthi, V. Impact of Oxidative and Osmotic Stresses on Candida Albicans Biofilm Formation. *Biofouling* **2016**, *32*, 897−909.
(84) Fonseca, E.; Silva, S.; Rodrigues, C. F.; Alves, C. T.; Azeredo, J.; Henriques, M. Effects of Fluconazole on Candida Glabrata Biofilms and Its Relationship with ABC Transporter Gene Expression. *Biofouling* **2014**, *30*, 447−457.
(85) Orta-Zavalza, E.; Briones-Martin-del-Campo, M.; Castano, I.; De Las Penas, A. Catalase Activity Assay in Candida Glabrata. *Bio-Protoc.* **2014**, *4*, No. e1072.
(86) Rajkowska, K.; Kunicka-Styczyńska, A.; Maroszyńska, M. Selected Essential Oils as Antifungal Agents against Antibiotic-Resistant Candida Spp.: In Vitro Study on Clinical and Food-Borne Isolates. *Microb. Drug Resist.* **2017**, *23*, 18−24.
(87) Kwolek-Mirek, M.; Zadrag-Tecza, R. Comparison of Methods Used for Assessing the Viability and Vitality of Yeast Cells. *FEMS Yeast Res.* **2014**, *14*, 1068−1079.
(88) Panwar, R.; Pemmaraju, S. C.; Sharma, A. K.; Pruthi, V. Efficacy of Ferulic Acid Encapsulated Chitosan Nanoparticles against Candida Albicans Biofilm. *Microb. Pathog.* **2016**, *95*, 21−31.
(89) Latifah-Munirah, B.; Himratul-Aznita, W. H.; Zain, N. M. Eugenol, an Essential Oil of Clove, Causes Disruption to the Cell Wall of Candida Albicans (ATCC 14053). *Front. Life Sci.* **2015**, *8*, 231−240.
(90) Kwolek-Mirek, M.; Zadrag-Tecza, R. Comparison of Methods Used for Assessing the Viability and Vitality of Yeast Cells. *FEMS Yeast Res.* **2014**, *14*, 1068−1079.
(91) Haque, F.; Alfatah, M.; Ganesan, K.; Bhattacharyya, M. S. Inhibitory Effect of Sophorolipid on Candida Albicans Biofilm Formation and Hyphal Growth. *Sci. Rep.* **2016**, *6*, 23575.
(92) Chandra, J.; Kuhn, D. M.; Mukherjee, P. K.; Hoyer, L. L.; McCormick, T.; Ghannoum, M. A. Biofilm Formation by the Fungal PathogenCandida Albicans: Development, Architecture, and Drug Resistance. *J. Bacteriol.* **2001**, *183*, 5385−5394.
(93) Imamura, Y.; Chandra, J.; Mukherjee, P. K.; Lattif, A. A.; Szczotka-Flynn, L. B.; Pearlman, E.; Lass, J. H.; O'Donnell, K.; Ghannoum, M. A. Fusarium and Candida Albicans Biofilms on Soft Contact Lenses: Model Development, Influence of Lens Type, and Susceptibility to Lens Care Solutions. *Antimicrob. Agents Chemother.* **2008**, *52*, 171−182.
(94) Singh, N.; Agrawal, V.; Pemmaraju, S. C.; Panwar, R.; Pruthi, V. Impact of Infectious Candida Albicans Biofilm on Biomaterials. *Indian J. Biotechnol.* **2011**, *10*, 417−422.

DOI: 10.1021/acsomega.8b01856
ACS Omega 2018, 3, 12201−12214